ATTITUDE STABILITY OF A SPINNING SYMMETRIC SATELLITE IN A PLANAR PERIODIC ORBIT

DONALD L. HITZL and DAVID A. LEVINSON

Lockheed Palo Alto Research Laboratory, Advanced Systems Studies, Dept. 52–56; Bldg. 201, 3251 Hanover St., Palo Alto, Calif., 94304, U.S.A.

(Received 23 June, 1978; accepted 6 February, 1979)

Abstract. This paper contains an analysis of the attitude stability of a spinning axisymmetric satellite whose mass center moves in any known planar periodic orbit of the restricted three-body problem while the spin axis remains normal to the orbit plane. A procedure based on Floquet theory is developed for constructing attitude instability charts, and examples of these are presented for two stable periodic orbits of the Earth–Moon system – one direct and one retrograde. The physical significance of these instability predictions is then explored by means of numerical integration of the full nonlinear equations of motion. Finally, an analysis based on averaging is performed, leading to approximate instability charts and indicating a possible connection between certain orbital-attitude resonance conditions and unstable attitude motions.

1. Introduction

Analysis of the attitude stability of orbiting rigid bodies has been a subject of considerable interest during the past two decades. Motivated by the need to design Earth-orbiting satellites of ever greater variety, early investigators in this area dealt primarily with bodies moving in circular or elliptic orbits. One such study was performed by DeBra and Delp (1961), who obtained explicit attitude stability criteria for an unsymmetric rigid body moving in a circular orbit about a particle. Later, Thomson (1962) and Kane *et al.* (1962) undertook an analysis of the effects of spin rate on the attitude stability of an axisymmetric satellite moving in a circular orbit with the satellite's spin axis normal to the orbit plane.

The symmetric satellite received further attention from Auelmann (1963) and Pringle (1964). Auelmann examined the stability of all of the equilibrium orientations of a 'nonspinning' satellite, that is, one whose inertial angular velocity vector has no component parallel to the spin axis, whereas Pringle studied the behavior of satellites not restricted by this requirement.

Kane and Shippy (1963) employed Floquet theory to test the stability of a spinning unsymmetric satellite moving in a circular orbit and having one central principal axis of inertia normal to the orbit plane. Kane (1965) then applied the same procedure to a stability analysis of Earth-pointing satellites, a subject which was subsequently explored in considerable detail with Hamiltonian methods by Breakwell and Pringle (1965).

Likins (1965) determined the complete set of cases where the axis of a spinning symmetric satellite in a circular orbit maintains a fixed orientation with respect to an

Celestial Mechanics **20** (1979) 179–205 0008-8714/79/0202-0179 $04.05.

orbiting reference frame and then examined the stability of each case. More recently, Hitzl (1972) investigated low-order resonant roll-yaw attitude instabilities for the case dealt with previously by Thomson (1962) and Kane *et al.* (1962).

Effects of orbital eccentricity on attitude stability were considered by a number of authors for a spinning, symmetric body traveling in an elliptic orbit with its spin axis normal to the orbit plane. Markeev (1965) examined the problem briefly, while Kane and Barba (1966) generated instability charts numerically using Floquet theory. Later, Markeev (1967a, b) studied the motion of the satellite's spin axis near conditions of low-order orbital-attitude resonance. Wallace and Meirovitch (1967), in contrast, treated the same problem with formal power series expansions valid for orbits of small eccentricity. Finally, in an investigation parallel to, but independent of Markeev (1967a), Hitzl (1970) analyzed this problem using the Hamiltonian methods developed by Breakwell and Pringle (1965).

All of the preceding references deal with the attitude motions of bodies whose mass centers move in simple circular or elliptic orbits about a single primary. However, many periodic orbits have been found for the restricted problem of *three* bodies during the past century. (For example, Szebehely (1967) lists more than one hundred references on this subject.) One is thus led to wonder how the attitude stability of, say, an axisymmetric spinning body is affected when its mass center traces out a periodic orbit of this type while its spin axis remains normal to the orbit plane. Kane and Marsh (1971) have already analyzed the special case where the body's center of mass is fixed at any one of the five equilibrium points of the restricted three-body problem.

In the present work, a procedure based on Floquet theory is developed for studying the stability of this same simple spinning motion for a satellite whose mass center moves in *any* known periodic orbit of the restricted problem. For illustrative purposes, several attitude instability charts are produced using recently discovered periodic orbits which are stable in the orbit plane (Hitzl and Hénon, 1977; Hitzl, 1977).

2. Analysis

The system to be analyzed (see Figure 1) consists of two particles, P_1 and P_2 and an axisymmetric rigid body B that move in a Newtonian reference frame N in which the mass center C of P_1 and P_2 is fixed. P_1 remains a constant distance l from P_2 while the line X connecting the particles rotates in N at a constant angular rate Ω. Lines Y and Z are perpendicular to X and pass through C, Y lying in the orbit plane of P_1 and P_2, and Z normal to this plane. The masses m_1 and m_2 of P_1 and P_2 are assumed to be so large in comparison with the mass m_3 of B that P_1 and P_2 are not influenced by the gravitational forces exerted on them by B, and we confine attention to motions of B during which its mass center B^* remains in the X-Y plane.

If R denotes the reference frame in which X and Y are fixed, then one can introduce a dextral set of mutually perpendicular unit vectors $\mathbf{r}_1$, $\mathbf{r}_2$, $\mathbf{r}_3$ fixed in R such

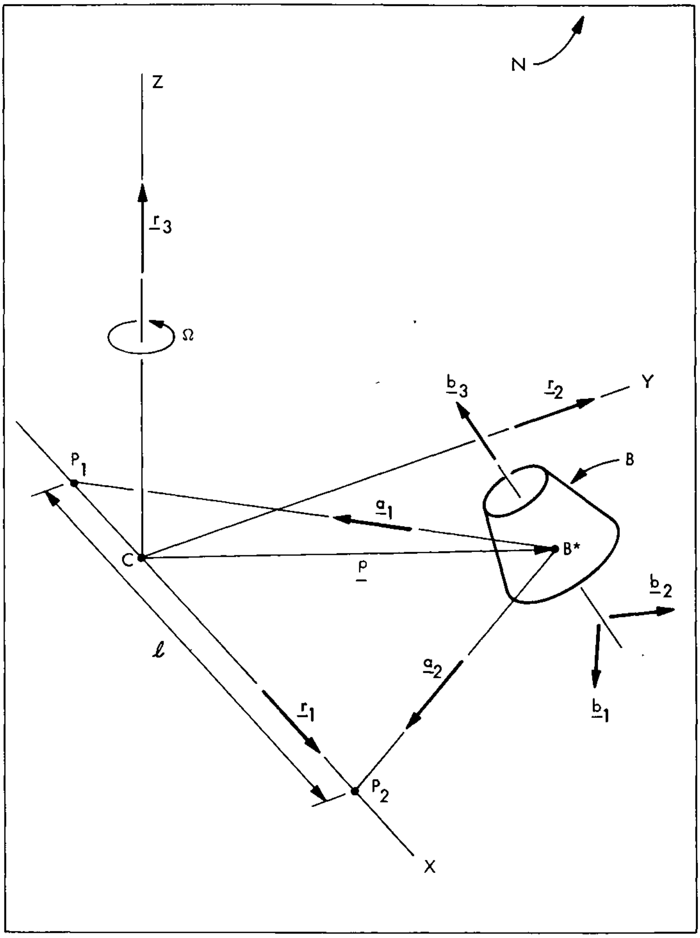

Fig. 1. Three-body system.

that $\mathbf{r}_1$ points from P_1 to P_2, $\mathbf{r}_2$ points in the direction of motion of P_2 in N, and $\mathbf{r}_3$ is parallel to Z with $\mathbf{r}_3 = \mathbf{r}_1 \times \mathbf{r}_2$. It is also convenient to introduce a second, similar, set of unit vectors $\mathbf{b}_1, \mathbf{b}_2, \mathbf{b}_3$ parallel to principal axes of inertia of B for B^*, with $\mathbf{b}_3$ parallel to the symmetry axis, as well as unit vectors $\mathbf{a}_1$ and $\mathbf{a}_2$ pointing from B^* to P_1 and P_2, respectively. Then one can express the position vector $\mathbf{p}$ of B^* relative to C, the angular velocity ${}^N\boldsymbol{\omega}^R$ of R in N, the angular velocity ${}^R\boldsymbol{\omega}^B$ of B in R, and the velocity ${}^N\mathbf{v}^{B^*}$ of B^* in N, as

$$\mathbf{p} = x\mathbf{r}_1 + y\mathbf{r}_2\,, \tag{1}$$

$$^N\boldsymbol{\omega}^R = \Omega\mathbf{r}_3\,, \tag{2}$$

$$^R\boldsymbol{\omega}^B = u_1\mathbf{b}_1 + u_2\mathbf{b}_2 + u_3\mathbf{b}_3\,, \tag{3}$$

$$^N\mathbf{v}^{B^*} = u_4\mathbf{r}_1 + u_5\mathbf{r}_2\,. \tag{4}$$

Since

$$^N\mathbf{v}^{B^*} = \frac{^R\mathrm{d}}{\mathrm{d}t}(\mathbf{p}) + {^N\boldsymbol{\omega}^R} \times \mathbf{p}\,, \tag{5}$$

where $^R\mathrm{d}/\mathrm{d}t$ denotes differentiation with respect to the time t in R, then substitution from Equations (1), (2) into Equation (5) and comparison with Equation (4) yields the kinematical equations

$$\dot{x} = u_4 + \Omega y\,, \tag{6}$$

$$\dot{y} = u_5 - \Omega x\,. \tag{7}$$

Next, the acceleration $^N\mathbf{a}^{B^*}$ of B^* in N, obtained from Equations (2), (4), and the relation

$$^N\mathbf{a}^{B^*} = \frac{^R\mathrm{d}}{\mathrm{d}t}(^N\mathbf{v}^{B^*}) + {^N\boldsymbol{\omega}^R} \times {^N\mathbf{v}^{B^*}} \tag{8}$$

can be written

$$^N\mathbf{a}^{B^*} = (\dot{u}_4 - \Omega u_5)\mathbf{r}_1 + (\dot{u}_5 + \Omega u_4)\mathbf{r}_2 \tag{9}$$

thus enabling one to construct the inertia force $\mathbf{F}^*$ acting on B, given by

$$\mathbf{F}^* = -m_3 {^N\mathbf{a}^{B^*}}\,. \tag{10}$$

In order to form the inertia torque $\mathbf{T}^*$ acting on B, it is first necessary to form an expression for the angular acceleration $^N\boldsymbol{\alpha}^B$ of B in N. This can be accomplished as follows: First note that

$$^N\boldsymbol{\alpha}^B = \frac{^B\mathrm{d}}{\mathrm{d}t}(^N\boldsymbol{\omega}^B)\,, \tag{11}$$

where $^N\boldsymbol{\omega}^B$ is the angular velocity of B in N, given by

$$^N\boldsymbol{\omega}^B = {^N\boldsymbol{\omega}^R} + {^R\boldsymbol{\omega}^B} \tag{12}$$

and $^B\mathrm{d}/\mathrm{d}t$ denotes differentiation with respect to t in B. Substitution from Equation (12) into Equation (11) then yields

$$^N\boldsymbol{\alpha}^B = \frac{^B\mathrm{d}}{\mathrm{d}t}(^N\boldsymbol{\omega}^R) + \frac{^B\mathrm{d}}{\mathrm{d}t}(^R\boldsymbol{\omega}^B)\,. \tag{13}$$

But,

$$\frac{^B\mathrm{d}}{\mathrm{d}t}(^N\boldsymbol{\omega}^R) = \frac{^R\mathrm{d}}{\mathrm{d}t}(^N\boldsymbol{\omega}^R) - {^R\boldsymbol{\omega}^B} \times {^N\boldsymbol{\omega}^R} \tag{14}$$

and, from Equation (2),

$$\frac{^R\mathrm{d}}{\mathrm{d}t}(^N\boldsymbol{\omega}^R) = 0\,. \tag{15}$$

Hence, Equations (13)–(15) yield the relation

$$ {}^N\boldsymbol{\alpha}^B = \frac{{}^B\mathrm{d}}{\mathrm{d}t}({}^R\boldsymbol{\omega}^B) - {}^R\boldsymbol{\omega}^B \times {}^N\boldsymbol{\omega}^R \tag{16} $$

so that, if one defines the direction cosines c_{ij} as

$$ c_{ij} \triangleq \mathbf{r}_i \cdot \mathbf{b}_j, \qquad (i, j = 1, 2, 3) \tag{17} $$

then substitution from Equations (2), (3) into Equation (16) gives

$$ \begin{aligned} {}^N\boldsymbol{\alpha}^B = {} & [\dot{u}_1 + \Omega(u_3c_{32} - u_2c_{33})]\mathbf{b}_1 + [\dot{u}_2 + \Omega(u_1c_{33} - u_3c_{31})]\mathbf{b}_2 + \\ & + [\dot{u}_3 + \Omega(u_2c_{31} - u_1c_{32})]\mathbf{b}_3 . \end{aligned} \tag{18} $$

In addition, substitution from Equations (2), (3) into Equation (12) produces

$$ {}^N\boldsymbol{\omega}^B = (u_1 + \Omega c_{31})\mathbf{b}_1 + (u_2 + \Omega c_{32})\mathbf{b}_2 + (u_3 + \Omega c_{33})\mathbf{b}_3 \tag{19} $$

so that one can construct $\mathbf{T}^*$ by substituting Equations (18), (19) into the definition (Kane, 1972, p. 116)

$$ \mathbf{T}^* \triangleq (\mathbf{I} \cdot {}^N\boldsymbol{\omega}^B) \times {}^N\boldsymbol{\omega}^B - \mathbf{I} \cdot {}^N\boldsymbol{\alpha}^B, \tag{20} $$

where $\mathbf{I}$, the inertia dyadic of B for B^*, is given by

$$ \mathbf{I} = J(\mathbf{b}_1\mathbf{b}_1 + \mathbf{b}_2\mathbf{b}_2) + I\mathbf{b}_3\mathbf{b}_3 . \tag{21} $$

The resulting expression is

$$ \begin{aligned} \mathbf{T}^* = {} & \{(u_2 + \Omega c_{32})(u_3 + \Omega c_{33})(J - I) - [\dot{u}_1 + \Omega(u_3c_{32} - u_2c_{33})]J\}\mathbf{b}_1 + \\ & + \{(u_3 + \Omega c_{33})(u_1 + \Omega c_{31})(I - J) - [\dot{u}_2 + \Omega(u_1c_{33} - u_3c_{31})]J\}\mathbf{b}_2 - \\ & - [\dot{u}_3 + \Omega(u_2c_{31} - u_1c_{32})]I\mathbf{b}_3 . \end{aligned} \tag{22} $$

Generalized inertia forces F_i^* associated with u_i $(i = 1, \ldots, 5)$ can then be constructed from $\mathbf{F}^*$, $\mathbf{T}^*$ (see Equations (10), (22)), and partial velocities $\partial {}^N\mathbf{v}^{B^*}/\partial u_i$ and partial angular velocities $\partial {}^N\boldsymbol{\omega}^B/\partial u_i$ $(i = 1, \ldots, 5)$ (see Equations (4), (19)), by means of the relation (Kane, 1972, pp. 44, 123)

$$ F_i^* = \frac{\partial {}^N\mathbf{v}^{B^*}}{\partial u_i} \cdot \mathbf{F}^* + \frac{\partial {}^N\boldsymbol{\omega}^B}{\partial u_i} \cdot \mathbf{T}^*, \qquad (i = 1, \ldots, 5) \tag{23} $$

which yields

$$ \left.\begin{aligned} F_1^* &= (u_2 + \Omega c_{32})(u_3 + \Omega c_{33})(J - I) - [\dot{u}_1 + \Omega(u_3c_{32} - u_2c_{33})]J, \\ F_2^* &= (u_3 + \Omega c_{33})(u_1 + \Omega c_{31})(I - J) - [\dot{u}_2 + \Omega(u_1c_{33} - u_3c_{31})]J, \\ F_3^* &= -[\dot{u}_3 + \Omega(u_2c_{31} - u_1c_{32})]I, \\ F_4^* &= -m_3(\dot{u}_4 - \Omega u_5), \\ F_5^* &= -m_3(\dot{u}_5 + \Omega u_4). \end{aligned}\right\} \tag{24} $$

Turning next to the determination of generalized active forces, we first introduce the position vectors $\mathbf{p}_1$ and $\mathbf{p}_2$ of P_1 and P_2 relative to B^*, given by

$$\left.\begin{aligned}\mathbf{p}_1 &= -[x + m_2 l/(m_1+m_2)]\mathbf{r}_1 - y\mathbf{r}_2\,,\\ \mathbf{p}_2 &= -[x - m_1 l/(m_1+m_2)]\mathbf{r}_1 - y\mathbf{r}_2\,.\end{aligned}\right\} \tag{25}$$

The assumption then is made that the largest dimension of B is 'very small' compared with l, so that the gravitational force $\mathbf{F}$ and gravitational torque $\mathbf{T}$ exerted on B by P_1 and P_2 may be written (Kane and Likins, 1975, pp. 14, 43)

$$\mathbf{F} = Gm_3(m_1\mathbf{a}_1/|\mathbf{p}_1|^2 + m_2\mathbf{a}_2/|\mathbf{p}_2|^2)\,, \tag{26}$$

$$\mathbf{T} = 3G[m_1(\mathbf{a}_1 \times \mathbf{I}\cdot\mathbf{a}_1)/|\mathbf{p}_1|^3 + m_2(\mathbf{a}_2 \times \mathbf{I}\cdot\mathbf{a}_2)/|\mathbf{p}_2|^3]\,. \tag{27}$$

Again making use of partial velocities and partial angular velocities, and, replacing $\mathbf{a}_i$ with $\mathbf{p}_i/|\mathbf{p}_i|$ $(i = 1, 2)$ (see Figure 1), one can obtain the generalized active forces $F_1, \ldots, F_5$ from the relationship

$$F_i = \frac{\partial^N\mathbf{v}^{B^*}}{\partial u_i}\cdot\mathbf{F} + \frac{\partial^N\boldsymbol{\omega}^B}{\partial u_i}\cdot\mathbf{T}, \qquad (i = 1, \ldots, 5). \tag{28}$$

By inserting Equations (4), (19), (26), (27) into Equation (28) we get

$$\left.\begin{aligned}F_1 &= 3G(m_1\rho_{12}\rho_{13}/|\mathbf{p}_1|^5 + m_2\rho_{22}\rho_{23}/|\mathbf{p}_2|^5)(I-J)\,,\\ F_2 &= 3G(m_1\rho_{13}\rho_{11}/|\mathbf{p}_1|^5 + m_2\rho_{23}\rho_{21}/|\mathbf{p}_2|^5)(J-I)\,,\\ F_3 &= 0\,,\\ F_4 &= -G\{m_1[x + m_2 l/(m_1+m_2)]/|\mathbf{p}_1|^3\\ &\qquad + m_2[x - m_1 l/(m_1+m_2)]/|\mathbf{p}_2|^3\}\,,\\ F_5 &= -G(m_1/|\mathbf{p}_1|^3 + m_2/|\mathbf{p}_2|^3)y\,,\end{aligned}\right\} \tag{29}$$

where G is the universal gravitational constant,

$$\rho_{1j} \triangleq -[x + m_2 l/(m_1+m_2)]c_{1j} - yc_{2j}\,, \qquad (j = 1, 2, 3) \tag{30}$$

$$\rho_{2j} \triangleq -[x - m_1 l/(m_1+m_2)]c_{1j} - yc_{2j}\,, \qquad (j = 1, 2, 3) \tag{31}$$

and, from Equations (25),

$$|\mathbf{p}_1| = [x + m_2 l/(m_1+m_2)]^2 + y^2\,, \tag{32}$$

$$|\mathbf{p}_2| = [x - m_1 l/(m_1+m_2)]^2 + y^2\,. \tag{33}$$

Dynamical equations of motion for this system are constructed via Kane's formulation (Kane, 1972, p. 177),

$$F_i^* + F_i = 0, \qquad (i = 1, \ldots, 5) \tag{34}$$

which, when employed in conjunction with Equations (24), (29), leads directly to

$$\left.\begin{aligned}
&(u_2+\Omega c_{32})(u_3+\Omega c_{33})(J-I)-[\dot{u}_1+\Omega(u_3c_{32}-u_2c_{33})]J+\\
&\quad+3G(m_1\rho_{12}\rho_{13}/|\mathbf{p}_1|^5+m_2\rho_{22}\rho_{23}/|\mathbf{p}_2|^5)(I-J)=0\,,\\
&(u_3+\Omega c_{33})(u_1+\Omega c_{31})(I-J)-[\dot{u}_2+\Omega(u_1c_{33}-u_3c_{31})]J+\\
&\quad+3G(m_1\rho_{13}\rho_{11}/|\mathbf{p}_1|^5+m_2\rho_{23}\rho_{21}/|\mathbf{p}_2|^5)(J-I)=0\,,\\
&\dot{u}_3+\Omega(u_2c_{31}-u_1c_{32})=0,\\
&m_3(\dot{u}_4-\Omega u_5)+G\{m_1[x+m_2l/(m_1+m_2)]/|\mathbf{p}_1|^3+\\
&\quad+m_2[x-m_1l/(m_1+m_2)]/|\mathbf{p}_2|^3\}=0\,,\\
&m_3(\dot{u}_5+\Omega u_4)+G(m_1/|\mathbf{p}_1|^3+m_2/|\mathbf{p}_2|^3)y=0\,.
\end{aligned}\right\}\qquad(35)$$

To complete the description of the motion of B, we let $\varepsilon_1, \ldots, \varepsilon_4$ be a set of Euler parameters characterizing the orientation of B in R, these being governed by the kinematical equations (Kane and Likins, 1971, pp. 119–120)

$$\left.\begin{aligned}
\dot{\varepsilon}_1&=\tfrac{1}{2}(u_1\varepsilon_4-u_2\varepsilon_3+u_3\varepsilon_2)\,,\\
\dot{\varepsilon}_2&=\tfrac{1}{2}(u_1\varepsilon_3+u_2\varepsilon_4-u_3\varepsilon_1)\,,\\
\dot{\varepsilon}_3&=\tfrac{1}{2}(-u_1\varepsilon_2+u_2\varepsilon_1+u_3\varepsilon_4)\,,\\
\dot{\varepsilon}_4&=-\tfrac{1}{2}(u_1\varepsilon_1+u_2\varepsilon_2+u_3\varepsilon_3)\,.
\end{aligned}\right\}\qquad(36)$$

Expressed in terms of $\varepsilon_1, \ldots, \varepsilon_4$, the direction cosines c_{ij} $(i, j=1, 2, 3)$ [see Equation (17)] become (Kane and Likins, 1971, p. 27)

$$\begin{aligned}
c_{ij}=2\varepsilon_i\varepsilon_j+\delta_{ij}\left(1-2\sum_{k=1}^{3}\varepsilon_k^2\right)-\\
-\sum_{k=1}^{3}(i-j)(j-k)(k-i)\varepsilon_k\varepsilon_4,\qquad(i, j=1, 2, 3),\qquad(37)
\end{aligned}$$

where δ_{ij} is the Kronecker delta.

The equations of motion can be put into nondimensional form by using the relation (Szebehely, 1967, p. 8) $G=\Omega^2l^3/(m_1+m_2)$ and defining the quantities $\mu\triangleq m_2/(m_1+m_2)$, $\bar{x}\triangleq x/l$, $\bar{y}\triangleq y/l$, $\bar{p}_i\triangleq|\mathbf{p}_i|/l$ $(i=1, 2)$, $\bar{\rho}_{ij}\triangleq\rho_{ij}/l$ $(i=1, 2;\ j=1, 2, 3)$, $\bar{u}_i\triangleq u_i/\Omega$ $(i=1, 2, 3)$, $\bar{u}_i\triangleq u_i/(\Omega l)$ $(i=4, 5)$, $\tau\triangleq\Omega t$, and $\nu\triangleq I/J$. Substituting these expressions into Equations (6), (7), (30)–(33), (35), (36) then gives

$$\left.\begin{aligned}
\bar{u}_1'&=(\bar{u}_2c_{33}-\bar{u}_3c_{32})+(1-\nu)\{(\bar{u}_2+c_{32})(\bar{u}_3+c_{33})-\\
&\quad-3[(1-\mu)\bar{\rho}_{12}\bar{\rho}_{13}/\bar{p}_1^5+\mu\bar{\rho}_{22}\bar{\rho}_{23}/\bar{p}_2^5]\}\,,\\
\bar{u}_2'&=(\bar{u}_3c_{31}-\bar{u}_1c_{33})-(1-\nu)\{(\bar{u}_3+c_{33})(\bar{u}_1+c_{31})-\\
&\quad-3[(1-\mu)\bar{\rho}_{13}\bar{\rho}_{11}/\bar{p}_1^5+\mu\bar{\rho}_{23}\bar{\rho}_{21}/\bar{p}_2^5]\}\,,\\
\bar{u}_3'&=\bar{u}_1c_{32}-\bar{u}_2c_{31}\,,
\end{aligned}\right\}\qquad(38)$$

$$\left.\begin{aligned}\bar{u}_4' &= \bar{u}_5 - (1-\mu)(\bar{x}+\mu)/\bar{p}_1^3 + \mu(-\bar{x}+1-\mu)/\bar{p}_2^3\,,\\ \bar{u}_5' &= -\bar{u}_4 - [(1-\mu)/\bar{p}_1^3 + \mu/\bar{p}_2^3]\bar{y}\,,\end{aligned}\right\} \tag{39}$$

$$\left.\begin{aligned}\varepsilon_1' &= \tfrac{1}{2}(\bar{u}_1\varepsilon_4 - \bar{u}_2\varepsilon_3 + \bar{u}_3\varepsilon_2)\,,\\ \varepsilon_2' &= \tfrac{1}{2}(\bar{u}_1\varepsilon_3 + \bar{u}_2\varepsilon_4 - \bar{u}_3\varepsilon_1)\,,\\ \varepsilon_3' &= \tfrac{1}{2}(-\bar{u}_1\varepsilon_2 + \bar{u}_2\varepsilon_1 + \bar{u}_3\varepsilon_4)\,,\\ \varepsilon_4' &= -\tfrac{1}{2}(\bar{u}_1\varepsilon_1 + \bar{u}_2\varepsilon_2 + \bar{u}_3\varepsilon_3)\,,\end{aligned}\right\} \tag{40}$$

$$\left.\begin{aligned}\bar{x}' &= \bar{u}_4 + \bar{y}\,,\\ \bar{y}' &= \bar{u}_5 - \bar{x}\,,\end{aligned}\right\} \tag{41}$$

where

$$\left.\begin{aligned}\bar{p}_1 &= [(\bar{x}+\mu)^2 + \bar{y}^2]^{1/2}\,,\\ \bar{p}_2 &= [(-\bar{x}+1-\mu)^2 + \bar{y}^2]^{1/2}\,,\\ &\left.\begin{aligned}\bar{\rho}_{1i} &= -(\bar{x}+\mu)c_{1i} - \bar{y}c_{2i}\,,\\ \bar{\rho}_{2i} &= (-\bar{x}+1-\mu)c_{1i} - \bar{y}c_{2i}\,,\end{aligned}\right\}\ (i=1,2,3)\end{aligned}\right\} \tag{42}$$

and the 'primes' denote differentiation with respect to the 'nondimensional time' τ.

Now, B can always perform a simple spinning motion in N during which $\mathbf{b}_3$ remains parallel to $\mathbf{r}_3$ and the angular velocity ${}^N\boldsymbol{\omega}^B$ is given by

$${}^N\boldsymbol{\omega}^B = \Gamma\mathbf{r}_3\,, \tag{43}$$

where Γ is a constant. Thus, if we define a 'nondimensional spin rate s of B in N' as $s \triangleq \Gamma/\Omega$, and let σ stand for the corresponding 'nondimensional spin rate of B in R', that is,

$$\sigma \triangleq s - 1 \tag{44}$$

then Equations (37), (38), (40), (42) are satisfied exactly by the solution $\bar{u}_1 = \bar{u}_2 = 0$, $\bar{u}_3 = \sigma$, $\varepsilon_1 = \varepsilon_2 = 0$, $\varepsilon_3 = \sin(\sigma\tau/2)$, $\varepsilon_4 = \cos(\sigma\tau/2)$, regardless of the τ-history of $\bar{u}_4$, $\bar{u}_5$, $\bar{x}$, and $\bar{y}$. It is the stability of this spinning motion that will now be investigated.

We begin by introducing perturbations $\xi_1, \ldots, \xi_7$, such that $\bar{u}_1 = \xi_1$, $\bar{u}_2 = \xi_2$, $\bar{u}_3 = \sigma + \xi_3$, $\varepsilon_1 = \xi_4$, $\varepsilon_2 = \xi_5$, $\varepsilon_3 = \sin(\sigma\tau/2) + \xi_6$, $\varepsilon_4 = \cos(\sigma\tau/2) + \xi_7$. Substituting these expressions into Equations (37), (38), (40), (42) and neglecting terms of second or higher degree in $\xi_1, \ldots, \xi_7$ produces the linearized variational system

$$\begin{aligned}&\xi_1' - \left[\xi_2 - 2\sigma\left(\xi_4\cos\frac{\sigma\tau}{2} + \xi_5\sin\frac{\sigma\tau}{2}\right)\right] -\\ &\quad -(\sigma+1)(1-\nu)\left[\xi_2 + 2\left(\xi_4\cos\frac{\sigma\tau}{2} + \xi_5\sin\frac{\sigma\tau}{2}\right)\right] -\\ &\quad -3(1-\nu)[h_1\eta_1\cos\sigma\tau - h_2(\eta_1\sin\sigma\tau + \eta_2\cos\sigma\tau) + h_3\eta_2\sin\sigma\tau] = 0\,,\end{aligned} \tag{45}$$

$$\xi_2' + \left[\xi_1 - 2\sigma\left(\xi_4 \sin\frac{\sigma\tau}{2} - \xi_5 \cos\frac{\sigma\tau}{2}\right)\right] +$$

$$+(\sigma+1)(1-\nu)\left[\xi_1 + 2\left(\xi_4 \sin\frac{\sigma\tau}{2} - \xi_5 \cos\frac{\sigma\tau}{2}\right)\right] +$$

$$+3(1-\nu)[h_1\eta_1 \sin\sigma\tau + h_2(\eta_1 \cos\sigma\tau - \eta_2 \sin\sigma\tau) - h_3\eta_2 \cos\sigma\tau] = 0\,, \tag{46}$$

$$\xi_3' = 0\,, \tag{47}$$

$$\xi_4' = \tfrac{1}{2}\left(\xi_1 \cos\frac{\sigma\tau}{2} - \xi_2 \sin\frac{\sigma\tau}{2} + \sigma\xi_5\right), \tag{48}$$

$$\xi_5' = \tfrac{1}{2}\left(\xi_1 \sin\frac{\sigma\tau}{2} + \xi_2 \cos\frac{\sigma\tau}{2} - \sigma\xi_4\right), \tag{49}$$

$$\xi_6' = \tfrac{1}{2}\left(\xi_3 \cos\frac{\sigma\tau}{2} + \sigma\xi_7\right), \tag{50}$$

$$\xi_7' = -\tfrac{1}{2}\left(\xi_3 \sin\frac{\sigma\tau}{2} + \sigma\xi_6\right), \tag{51}$$

where

$$h_1 \triangleq \left(\frac{1-\mu}{\bar{p}_1^5} + \frac{\mu}{\bar{p}_2^5}\right)\bar{y}^2\,, \tag{52}$$

$$h_2 \triangleq \left[\frac{1-\mu}{\bar{p}_1^5}(\bar{x}+\mu) + \frac{\mu}{\bar{p}_2^5}(\bar{x}+\mu-1)\right]\bar{y}\,, \tag{53}$$

$$h_3 \triangleq \frac{1-\mu}{\bar{p}_1^5}(\bar{x}+\mu)^2 + \frac{\mu}{\bar{p}_2^5}(\bar{x}+\mu-1)^2\,, \tag{54}$$

$$\eta_1 \triangleq 2\left(\xi_4 \cos\frac{\sigma\tau}{2} - \xi_5 \sin\frac{\sigma\tau}{2}\right), \tag{55}$$

$$\eta_2 \triangleq 2\left(\xi_4 \sin\frac{\sigma\tau}{2} + \xi_5 \cos\frac{\sigma\tau}{2}\right). \tag{56}$$

Equations (47), (50), (51) involve only ξ_3, ξ_6, ξ_7 and, hence, are independent of Equations (45), (46), (48), (49). If $\xi_i(0)$ denotes the value of ξ_i ($i = 3, 6, 7$) at $\tau = 0$, then Equations (47), (50), (51) may be integrated in literal form to give

$$\xi_3 = \xi_3(0)\,, \tag{57}$$

$$\xi_6 = \xi_6(0) \cos\frac{\sigma\tau}{2} + \left[\frac{\xi_3(0)}{\sigma} + \xi_7(0)\right] \sin\frac{\sigma\tau}{2}\,, \tag{58}$$

$$\xi_7 = \frac{2}{\sigma}\,\xi_3(0)\left(\cos\frac{\sigma\tau}{2} - 1\right) - \xi_6(0) \sin\frac{\sigma\tau}{2} + \xi_7(0) \cos\frac{\sigma\tau}{2}\,, \tag{59}$$

which reveals that ξ_3, ξ_6, ξ_7 are all periodic functions of τ and thus cannot become unbounded as $\tau \to \infty$. The remaining equations, (45), (46), (48), (49), can be further simplified by noting that if η_3 and η_4 are defined as

$$\eta_3 \triangleq \xi_1 \cos \sigma\tau - \xi_2 \sin \sigma\tau\,, \tag{60}$$

$$\eta_4 \triangleq \xi_1 \sin \sigma\tau + \xi_2 \cos \sigma\tau \tag{61}$$

then, from Equations (48), (49), (55), (56), we find that

$$\eta_1' = \eta_3 \tag{62}$$

$$\eta_2' = \eta_4 \tag{63}$$

and Equations (45), (46), (55), (56) give

$$\eta_3' = -H_1\eta_4 - H_2\eta_1 + H_3(h_1\eta_1 - h_2\eta_2)\,, \tag{64}$$

$$\eta_4' = H_1\eta_3 - H_2\eta_2 + H_3(h_3\eta_2 - h_2\eta_1)\,, \tag{65}$$

where (see Equation (44))

$$H_1 = s\nu - 2\,, \tag{66}$$

$$H_2 = s\nu - 1\,, \tag{67}$$

$$H_3 = 3(1-\nu)\,. \tag{68}$$

Equations (62)–(65) are linear in the variables $\eta_1, \ldots, \eta_4$, but contain coefficients h_1, h_2, h_3 which are nonlinear functions of the variables $\bar{x}$, $\bar{y}$ (see Equations (52)–(54)) characterizing the position of B^* in N. Hence, if the 'orbit equations', Equations (39), (41), are numerically integrated using any set of initial values for $\bar{x}$, $\bar{y}$, $\bar{u}_4$, $\bar{u}_5$ known to produce a periodic orbit, the resulting solution can be combined with Equations (62)–(65) to form a linearized variational system with periodic coefficients, and Floquet theory can then be used to study the attitude stability of B in N for the simple spin under consideration. The algorithm that follows may be employed for this purpose.

3. Algorithm

(1) Input values of μ, s, ν, where $0 < \mu \leq \frac{1}{2}$, $-\infty < s < \infty$, $0 \leq \nu \leq 2$.
(2) Input initial values $\bar{x}(0)$, $\bar{y}(0)$, $\bar{x}'(0)$, $\bar{y}'(0)$ of $\bar{x}$, $\bar{y}$, $\bar{x}'$, $\bar{y}'$ which are known to produce a periodic orbit. Input the nondimensional period τ^* of the orbit.
(3) Compute H_1, H_2, H_3 from Equations (66)–(68).
(4) Define $W_1, \ldots, W_{20}$ as follows:

$$W_i \triangleq \begin{cases} 1, & i = 1, 6, 11, 16 \\ 0, & i = 2, \ldots, 15;\, i \neq 6, 11 \end{cases}$$

$$W_{17} \triangleq \bar{x}'(0) - \bar{y}(0)\,, \qquad W_{18} \triangleq \bar{y}'(0) + \bar{x}(0)$$

$$W_{19} = \bar{x}(0)\,, \qquad W_{20} = \bar{y}(0)\,.$$

(5) Form $X_1, X_2, \bar{p}_1, \bar{p}_2, g_{13}, g_{23}, g_{15}, g_{25}, h_1, h_2, h_3$ as

$$X_1 = W_{19} + \mu,$$
$$X_2 = X_1 - 1,$$
$$\bar{p}_1 = (X_1^2 + W_{20}^2)^{1/2},$$
$$\bar{p}_2 = (X_2^2 + W_{20}^2)^{1/2},$$
$$g_{13} \triangleq (1-\mu)/\bar{p}_1^3, \qquad g_{23} \triangleq \mu/\bar{p}_2^3,$$
$$g_{15} \triangleq g_{13}/\bar{p}_1^2, \qquad g_{25} \triangleq g_{23}/\bar{p}_2^2,$$
$$h_1 = (g_{15} + g_{25}) W_{20}^2,$$
$$h_2 = (g_{15} X_1 + g_{25} X_2) W_{20},$$
$$h_3 = g_{15} X_1^2 + g_{25} X_2^2.$$

(6) Perform a numerical integration from $\tau = 0$ to $\tau = \tau^*$ of the following twenty first-order differential equations:

$$\left.\begin{aligned}
W_i' &= W_{i+2}, \\
W_{i+1}' &= W_{i+3}, \\
W_{i+2}' &= -H_1 W_{i+3} - H_2 W_i + H_3(h_1 W_i - h_2 W_{i+1}), \\
W_{i+3}' &= H_1 W_{i+2} - H_2 W_{i+1} + \\
&\qquad + H_3(h_3 W_{i+1} - h_2 W_i),
\end{aligned}\right\} \qquad (i = 1, 5, 9, 13)$$

$$W_{17}' = W_{18} - (g_{13} X_1 + g_{23} X_2),$$
$$W_{18}' = -W_{17} - (g_{13} + g_{23}) W_{20},$$
$$W_{19}' = W_{17} + W_{20},$$
$$W_{20}' = W_{18} - W_{19}.$$

(7) Form the matrix D whose elements D_{ij} are given by $D_{ij} = W_{i+4j-4}^*$ $(i, j = 1, \dots, 4)$, where W_l^* denotes the value of W_l $(l = 1, \dots, 16)$ evaluated at $\tau = \tau^*$.

(8) Compute the eigenvalues $\lambda_1, \dots, \lambda_4$ of D.

(9) Compute the modulus Q_i of λ_i $(i = 1, \dots, 4)$.

(10) The motion of interest is unstable if $Q_i > 1$ for *any* i $(i = 1, \dots, 4)$.

(Whereas an *instability* prediction based on an analysis of linearized equations holds for the corresponding nonlinear equations, the converse is not necessarily true. That is, a *stability* prediction obtained from linearized equations does not always apply to the original nonlinear problem. For this reason, since Equations (62)–(65) were obtained by linearization, stability cannot be concluded if $Q_i \leqslant 1$ $(i = 1, \dots, 4)$.)

4. Application

Before the algorithm was used to generate any new results, it was subjected to extensive testing. First, instability predictions produced by the algorithm were checked against those published previously by Kane *et al.* (1962), Markeev (1967a), Wallace and Meirovitch (1967), and Hitzl (1970, 1972), for the case where the satellite moves in a circular orbit about a single primary. This was accomplished by setting $\mu = 0$, $\bar{x}(0) = 1$, $\bar{y}(0) = \bar{x}'(0) = \bar{y}'(0) = 0$, $\tau^* = 2\pi$, and executing the algorithm repeatedly using each of the 81 pairs of values of ν and s taken from the following sets:

$$\nu = 0.00, 0.25, 0.50, \ldots 2.00\,,$$

$$s = -2.0, -1.5, -1.0, \ldots 2.0\,.$$

Agreement with the references cited was obtained in each instance.

Next, the algorithm was applied to a stability analysis of a satellite whose mass center is located at the equilibrium point L_4 of the restricted three-body problem by taking $\mu = \mu^* \triangleq 0.012\,150\,67$ (corresponding to the Earth–Moon system (Hitzl, 1977)), $\bar{x}(0) = 0.5 - \mu$, $\bar{y}(0) = \sqrt{3}/2$, $\bar{x}'(0) = \bar{y}'(0) = 0$, and $\tau^* = 2\pi$. Using the same set of values for ν and s as in the first test, the algorithm produced results consistent with those of Kane and Marsh (1971). Moreover, in both tests, the values of $\bar{x}$, $\bar{y}$, $\bar{x}'$, $\bar{y}'$ computed at $\tau = \tau^*$ were found to agree to six significant figures with the input quantities $\bar{x}(0)$, $\bar{y}(0)$, $\bar{x}'(0)$, $\bar{y}'(0)$, respectively, thus verifying that the orbits did, indeed, 'close'.

After these successful tests were completed, instability charts were generated for two new cases – one where the mass center of the satellite travels in a stable direct periodic orbit of family C_{12} (Hitzl and Hénon, 1977) for the Earth–Moon system, and one where the mass center moves in a stable retrograde orbit of the same family. These instability charts are shown in Figures 2 and 3 next to plots of the corresponding orbits. The algorithm was applied using each of the values of ν and s that lie at an intersection of the grid lines shown, with points found to be unstable each being denoted by a cross. The orbits were produced using, for the direct orbit, the input quantities

$$\bar{x}(0) = 1.020\,757\,821\,745\,871\,3\,,$$

$$\bar{y}(0) = \bar{x}'(0) = 0.0\,,$$

$$\bar{y}'(0) = -1.011\,745\,634\,924\,788\,4\,,$$

$$\tau^* = 5.577\,015\,533\,806\,797\,8\,,$$

and, for the retrograde orbit,

$$\bar{x}(0) = 1.0014\,,$$

$$\bar{y}(0) = \bar{x}'(0) = 0.0\,,$$

$$\bar{y}'(0) = -2.287\,843\,199\,244\,397\,6\,,$$

$$\tau^* = 7.860\,726\,736\,662\,694\,6\,.$$

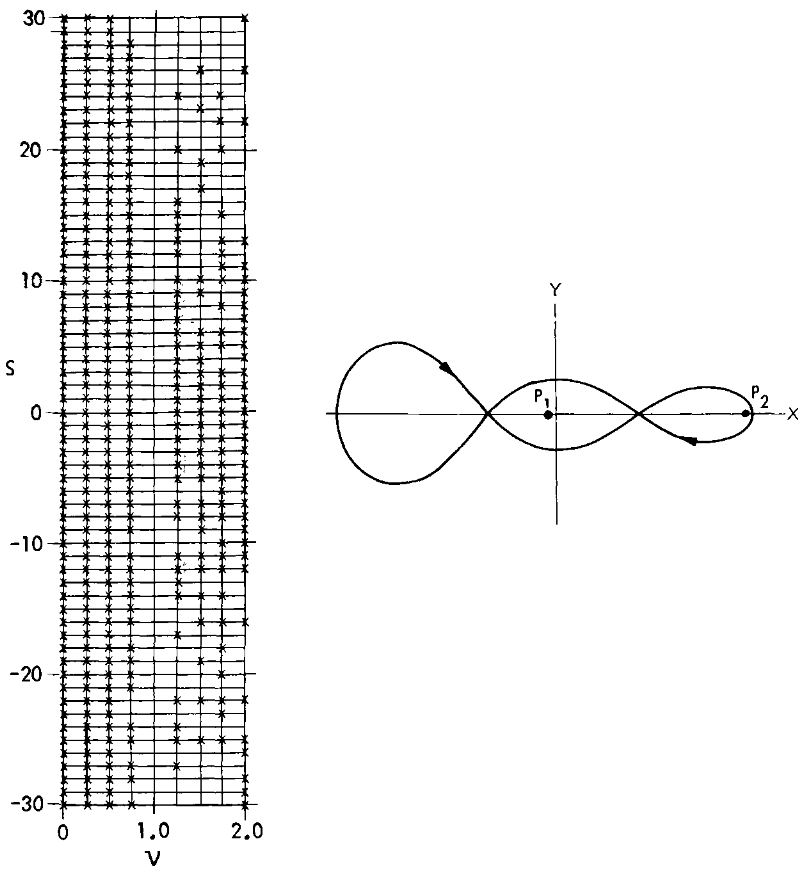

Fig. 2. Attitude instability chart for a stable direct orbit of family C_{12}.

One of the more striking features of the charts is that the profusion of unstable points is much greater in Figure 3 than in Figure 2 although, for the values of s considered, all points in Figure 2 for $\nu = 0.25$ and $\nu = 0.50$ are unstable while, in Figure 3 for these values of ν, there are five points that are not unstable. Because of the abundance of unstable points, the present charts resemble those obtained previously by Kane and Barba (1966) for a satellite moving in an elliptic orbit of high eccentricity about a single primary. However, one can see that much higher nondimensional spin rates must be employed to avoid unstable attitude motions in these orbits than are required in the two-body case. This situation arises from the fact that one revolution per minute corresponds approximately to $s = 100$ in the case of a satellite orbiting the Earth while, for a satellite moving in Earth–Moon orbits of the types considered in this paper, one revolution per minute is roughly equivalent to $s = 40\,000$. Thus, for Earth–Moon orbits with $|s| \leqslant 30$, one would expect unstable attitude motions to be prevalent.

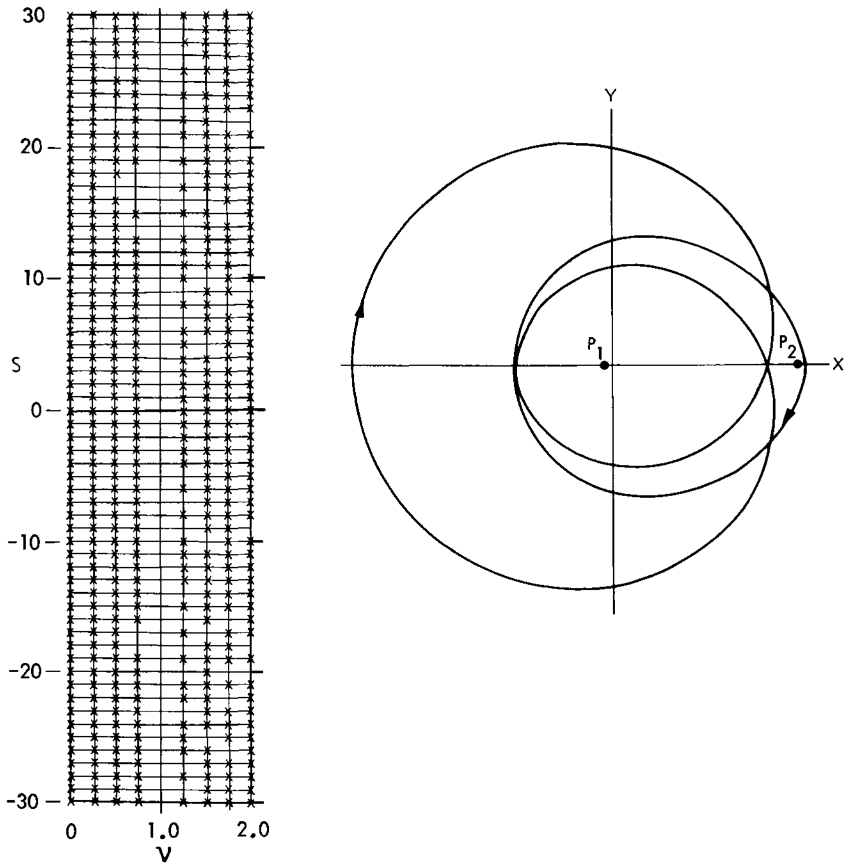

Fig. 3. Attitude instability chart for a stable retrograde orbit of family C_{12}.

The instability charts of Figures 2 and 3 exhibit a rather complex structure, that is, it is not a simple matter to construct curves on either chart that separate regions composed only of unstable points from regions containing no unstable points. To explore this state of affairs further, we produced an enlargement of the chart in Figure 2 in the vicinity of the apparently isolated unstable point at $\nu = 1.25$, $s = 20$. In this enlargement, shown in Figure 4, the region closely surrounding $\nu = 1.25$, $s = 20$ is seen to possess many unstable points which were not revealed in Figure 2. Furthermore, with the exception of what appears to be a solid region in its lower left corner, Figure 4 displays a structure having about the same degree of complexity as that found in Figure 2. Figure 5a shows a second enlargement of Figure 2 in the vicinity of $\nu = 1.25$, $s = 20$. At this magnification, there is a clearly defined unstable band passing diagonally across the chart.

One might wonder how a portion of Figure 4 which contains no unstable points would look under increased magnification. An enlargement of the region near $\nu = 1.24$, $s = 20.5$ is shown in Figure 5b. One can see that, far from being free of

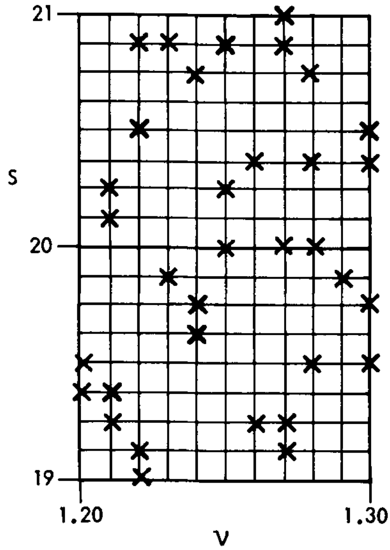

Fig. 4. Enlargement of a portion of the instability chart shown in Figure 2 in the vicinity of $\nu = 1.25$, $s = 20$.

unstable points, the region possesses a diagonal band of instability as well as a concentration of unstable points in the upper right corner.

Returning now to the apparently solid unstable region in the lower left corner of Figure 4, one finds from an enlargement of the vicinity of $\nu = 1.21$, $s = 19.3$ that the region actually is made up of two unstable bands separated by a band containing no unstable points. Finally, an enlargement of Figure 5c near $\nu = 1.21$, $s = 19.35$, shown in Figure 6, reveals that the basic structure of the instability chart shown in Figure 2 becomes discernible at the level of magnification used in Figures 5a–c. That is, the complexity of the structure does not increase with further magnification. Thus we see that the chart in Figure 2 is composed in part of diagonal instability bands having various widths.

Satellites having nondimensional spin rates in the range $0 \leqslant s \leqslant 0.1$ are of practical interest since the rate $s = \frac{1}{12} = 0.0833\ldots$ corresponds approximately to one rotation per year, this being the rate at which a satellite travelling in an Earth–Moon orbit would have to rotate in order to keep its solar panels oriented toward the Sun. For the case $s = \frac{1}{12}$, the values of ν giving rise to unstable spins lie in the ranges

$$0 \leqslant \nu \leqslant 0.9975\,, \qquad 1.01 \leqslant \nu \leqslant 1.02\,, \qquad 1.0375 \leqslant \nu \leqslant 2.0\,.$$

Now, one can justifiably ask, "How does the actual perturbed attitude motion of a satellite whose stability is characterized by a cross on an instability chart differ from the perturbed motion of a satellite whose motion is not characterized by a cross?" To answer this question, the full nonlinear equations of motion, Equations (38)–(42), were solved numerically. First, attention was focused on the unstable point in Figure

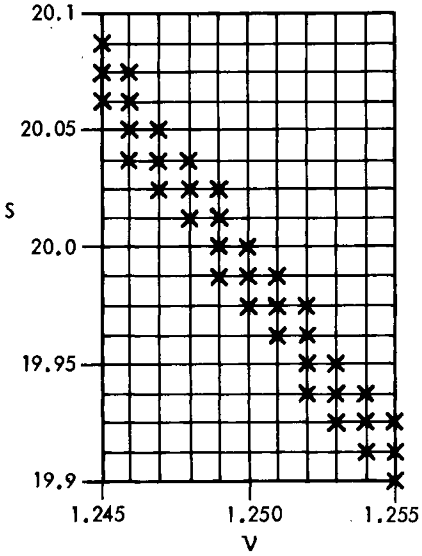

Fig. 5a. A second enlargement of Figure 2 in the vicinity of $\nu = 1.25$, $s = 20.0$.

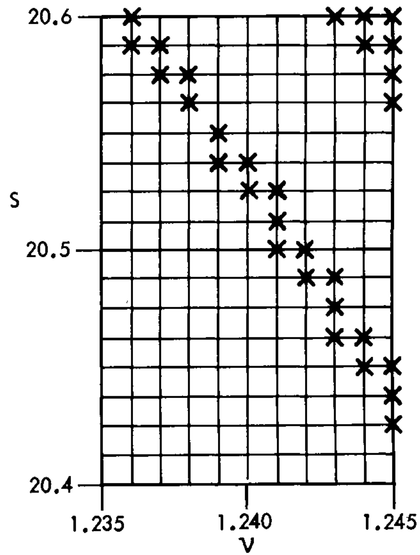

Fig. 5b. A second enlargement of a region of Figure 2 in the vicinity of $\nu = 1.24$, $s = 20.5$ which, in Figure 4, apparently contains no unstable points.

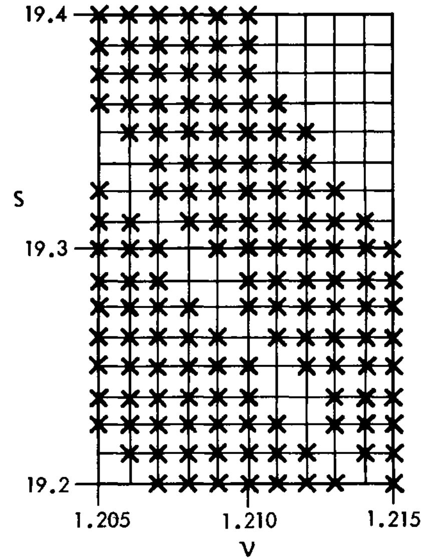

Fig. 5c. A second enlargement of a region of Figure 2 in the vicinity of $\nu = 1.21$, $s = 19.3$ which, in Figure 4, apparently contains a single instability band.

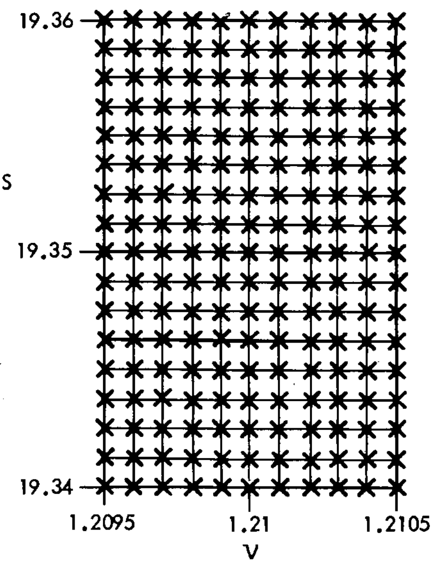

Fig. 6. An enlargement of Figure 5c in the vicinity of $\nu = 1.21$, $s = 19.35$.

2 at $\nu = 0.75$, $s = 7$. For initial conditions, we used the values of $\bar{x}(0)$, $\bar{y}(0)$, $\bar{x}'(0)$, $\bar{y}'(0)$ employed previously to construct Figure 2, chose

$\bar{u}_3(0) = s - 1 = 6\,,$ (see Equation (44))

$\bar{u}_2(0) = 0\,,$

$\bar{u}_1(0) = \bar{u}_3(0)/10 = 0.6\,,$ (This value constitutes a perturbation of the simple spin under consideration.)

$$\left.\begin{aligned} \bar{u}_4(0) &= \bar{x}'(0) - \bar{y}(0)\,, \\ \bar{u}_5(0) &= \bar{y}'(0) + \bar{x}(0)\,, \end{aligned}\right\} \quad \text{(see Equations (41))}$$

$\varepsilon_1(0) = \varepsilon_2(0) = \varepsilon_3(0) = 0\,,$ $\varepsilon_4(0) = 1\,,$

and then solved Equations (38)–(42) to produce a plot of the 'nutation angle' θ between the satellite's spin axis and the orbit normal as a function of the number of satellite orbits τ/τ^*. This angle was determined using the expression (see Figure 1 and Equations (17), (37))

$$\theta \triangleq \cos^{-1}(\mathbf{b}_3 \cdot \mathbf{r}_3) = \cos^{-1}(c_{33})\,. \tag{69}$$

The resulting curve is displayed in Figure 7a, from which it can be seen that θ attains peak values of more than 100° in less than one orbit. Now one might conclude that this growth is the direct result of an excessively large initial perturbation. To see that this is not the case, one need only examine Figures 7b and 7c, which were produced with the same input values as was Figure 7a, except that for Figure 7b, $\bar{u}_1(0) = 0.12$ (one fifth of its original value), and for Figure 7c, $\bar{u}_1(0) = 0.06$ (one tenth of its

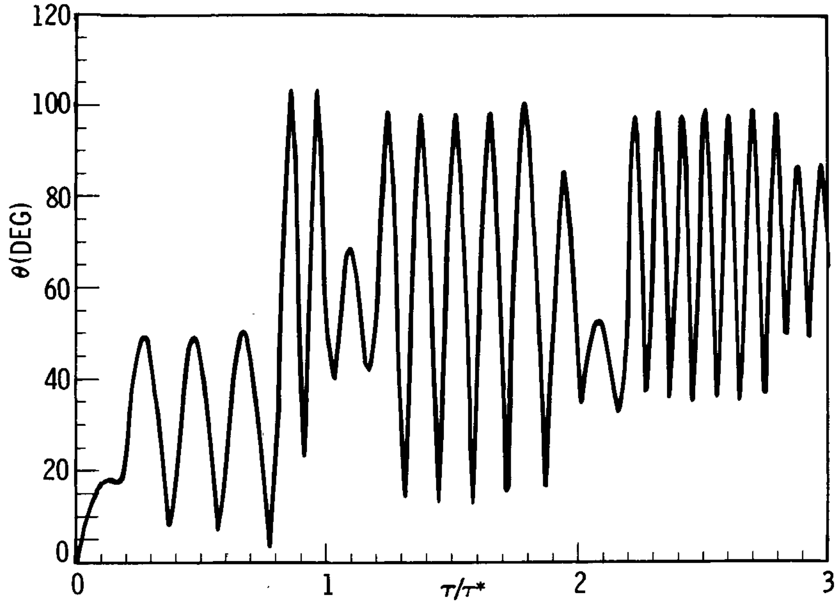

Fig. 7a. $\nu = 0.75$, $s = 7$, $\bar{u}_1(0) = 0.6$.

Fig. 7a–f. Attitude behavior of the spin axis.

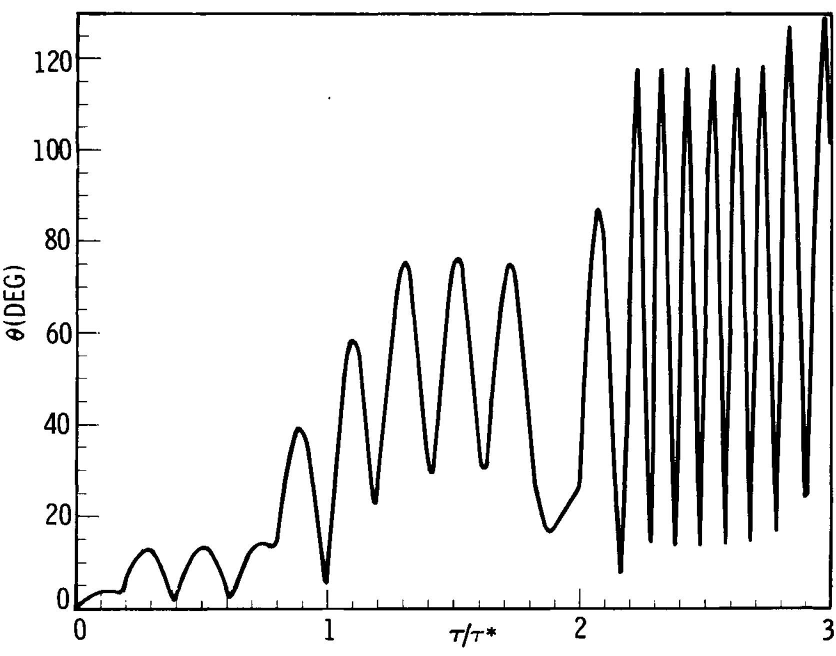

Fig. 7b. $\nu = 0.75$, $s = 7$, $\bar{u}_1(0) = 0.12$.

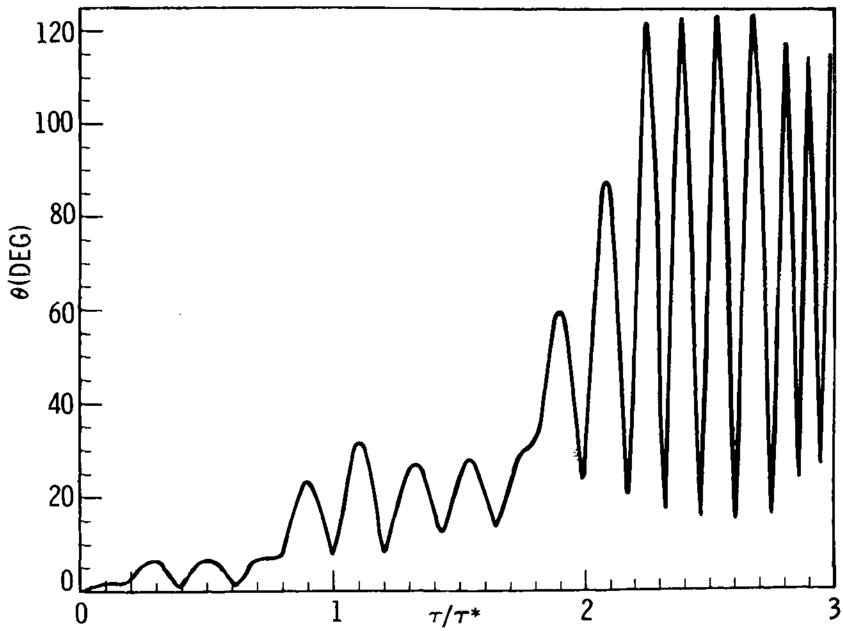

Fig. 7c. $\nu = 0.75$, $s = 7$, $\bar{u}_1(0) = 0.06$.

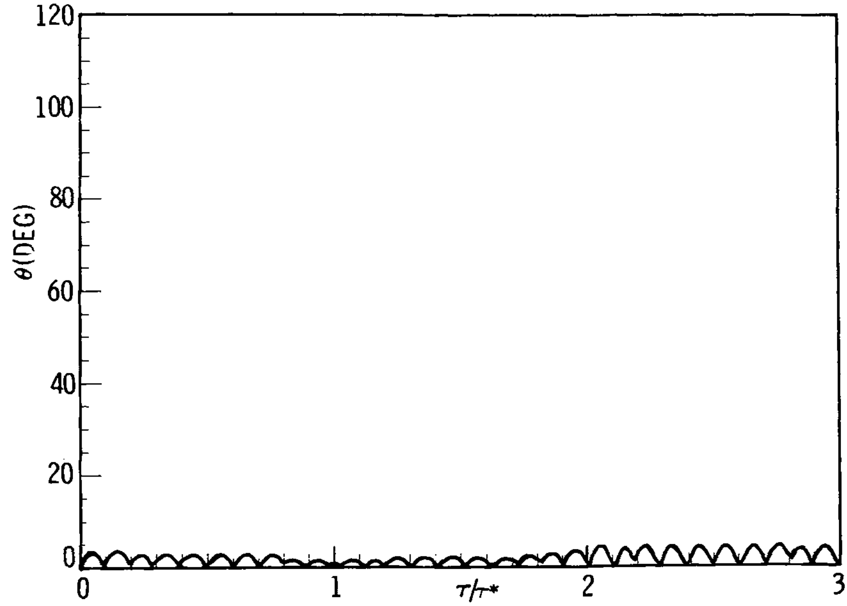

Fig. 7d. $\nu = 1.5$, $s = 7$, $\bar{u}_1(0) = 0.6$.

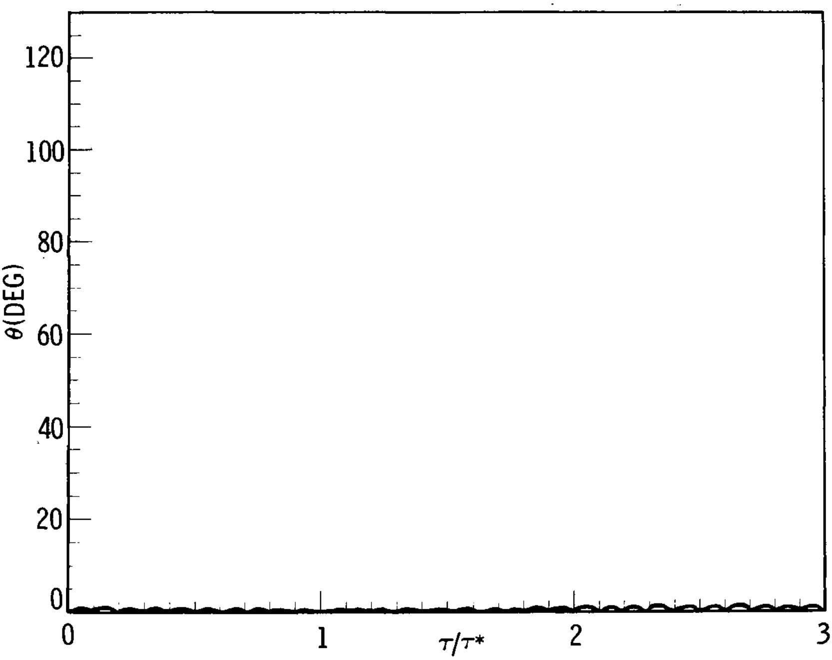

Fig. 7e. $\nu = 1.5$, $s = 7$, $\tilde{u}_1(0) = 0.12$.

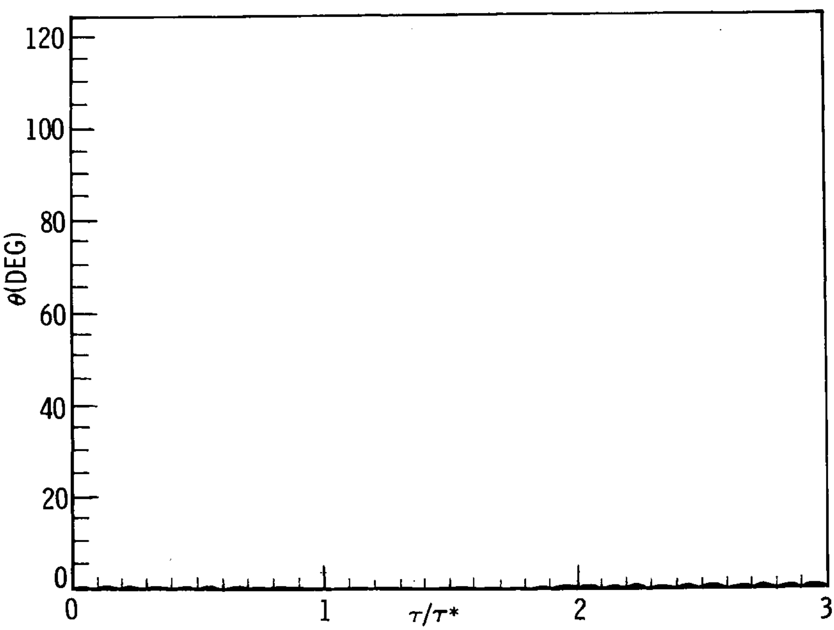

Fig. 7f. $\nu = 1.5$, $s = 7$, $\tilde{u}_1(0) = 0.06$.

original value). In both of these cases, the oscillations in θ build up to values exceeding those in Figure 7a, although they require somewhat longer to do so.

Figures 7d, 7e, and 7f contain curves which were generated with exactly the same initial conditions as those used to produce Figures 7a, 7b, and 7c, respectively, except that the value of ν was increased from 0.75 to 1.5, this new value corresponding to a point in the instability chart of Figure 2 that is not characterized by a cross. In this case, a decrease in the size of the initial perturbation is accompanied by a decrease in the peak values of θ, thus illustrating the fundamental difference between unstable and stable motions.

5. Approximations

In an attempt to shed further light on the results just presented for the direct orbit of family C_{12}, an approximate analysis based on averaging is undertaken in this section.

Floquet theory is required to generate the instability charts presented in Figures 2–6 only because the periodic nature of the coefficients h_1, h_2, h_3 in the variational equations (64) and (65) precludes one from using existing analytical techniques that have been developed for the stability analysis of linearized variational systems with *constant* coefficients. However, if h_i is replaced with a corresponding constant value $\tilde{h}_i$ formed by 'averaging' h_i over one orbit according to the definition

$$\tilde{h}_i \triangleq (1/\tau^*) \int_0^{\tau^*} h_i \, \mathrm{d}\tau, \qquad (i = 1, 2, 3), \tag{70}$$

then Equations (62)–(65) lend themselves readily to the analytical techniques just mentioned. In particular, approximate results found by averaging then can be compared with exact results obtained previously using Floquet theory.

First, we note that if a periodic orbit is symmetric with respect to the X-axis, then $\bar{x}$ and $\bar{y}$ are, respectively, even and odd functions of τ. Hence, the right-hand side of Equation (53) is an odd function of τ so that $\tilde{h}_2$ is identically zero. Since all of the orbits considered in this paper satisfy this symmetry condition, we can write 'averaged' versions of Equations (64) and (65) as

$$\begin{aligned} \eta_3' &= -H_1\eta_4 - H_2\eta_1 + H_3\tilde{h}_1\eta_1, \\ \eta_4' &= H_1\eta_3 - H_2\eta_2 + H_3\tilde{h}_3\eta_2. \end{aligned} \tag{71}$$

Combining these equations with Equations (62) and (63) yields

$$\begin{aligned} &\eta_1'' + H_1\eta_2' + (H_2 - H_3\tilde{h}_1)\eta_1 = 0, \\ &\eta_2'' - H_1\eta_1' + (H_2 - H_3\tilde{h}_3)\eta_2 = 0, \end{aligned} \tag{72}$$

which can be thought of as perturbation equations characterizing the spin axis attitude motion over many orbits. [So far, no physical significance has been attributed to the variables $\eta_1, \ldots, \eta_4$, but they can be given meaning as follows. The spin axis of the satellite B (see Figure 1) can be brought into a general orientation in reference frame R by first aligning $\mathbf{b}_i$ with $\mathbf{r}_i$ ($i = 1, 2, 3$) and then subjecting B to two successive rotations in R characterized by $\theta_1\mathbf{b}_1$ and $\theta_2\mathbf{b}_2$. The simple spin of interest then takes place in the reference state $\theta_1 = \theta_2 = 0$. The quantities η_1 and η_2 given in Equations (55) and (56) can be shown to represent, respectively, perturbations $\delta\theta_1$ and $\delta\theta_2$ relative to this state, while η_3 and η_4, defined in Equations (60) and (61), are precisely $\delta\theta_1'$ and $\delta\theta_2'$. Also, setting $\mu = \bar{y} = 0$ and $\bar{x} = 1$ in Equations (52)–(54), we find that Equations (62)–(65) reduce to the perturbation equations obtained previously for a symmetric satellite in a circular orbit (Hitzl, 1972).]

Next, we assume that solutions of Equations (72) are of the form

$$\eta_i = A_i e^{\omega t}, \qquad (i = 1, 2), \tag{73}$$

where A_1, A_2, and ω are constants, which leads to the characteristic equation

$$\omega^4 + \beta\omega^2 + \gamma = 0 \tag{74}$$

with

$$\begin{aligned} \beta &= H_1^2 + 2H_2 - H_3(\tilde{h}_1 + \tilde{h}_3)\,, \\ \gamma &= H_2^2 - H_2H_3(\tilde{h}_1 + \tilde{h}_3) + H_3^2\tilde{h}_1\tilde{h}_3\,. \end{aligned} \tag{75}$$

Equation (74) must have at least one root with a positive real part if

$$\beta < 0 \quad \text{or} \quad \gamma < 0 \quad \text{or} \quad \beta^2 - 4\gamma < 0 \tag{76}$$

that is, unstable attitude motions are guaranteed whenever one of conditions (76) is satisfied.

Now, once numerical values of $\tilde{h}_1$ and $\tilde{h}_3$ have been computed for a particular orbit, approximate instability regions can be determined using inequalities (76). The values of μ, $\bar{x}(0)$, $\bar{y}'(0)$, and τ^* used in the preceding section lead to, for the direct orbit,

$$\tilde{h}_1 = 7.830\,576\,, \qquad \tilde{h}_3 = 9.419\,220$$

and, for the retrograde orbit,

$$\tilde{h}_1 = 4.520\,160\,, \qquad \tilde{h}_3 = 6.400\,799\,.$$

Approximate instability charts obtained for these two orbits are shown in Figure 8, where the shaded regions correspond to instability. Comparison of these charts with their 'exact' counterparts in Figures 2 and 3 reveals that, with only a few exceptions, a (ν, s) pair predicted to be unstable in Figure 8 is also found to be unstable using the Floquet method. However, as might be expected, the charts in Figure 8 fail completely to delineate the complicated zones of instability found previously for $\nu \geqslant 1.2$.

Next, an attempt was made to correlate the diagonal bands of instability shown in Figures 5a–c with the occurrence of certain resonance regions in the $\nu - s$ plane. For an orbit of small eccentricity about a single primary, 'external resonance' is said to occur when either of the two frequencies of spin axis oscillations is nearly

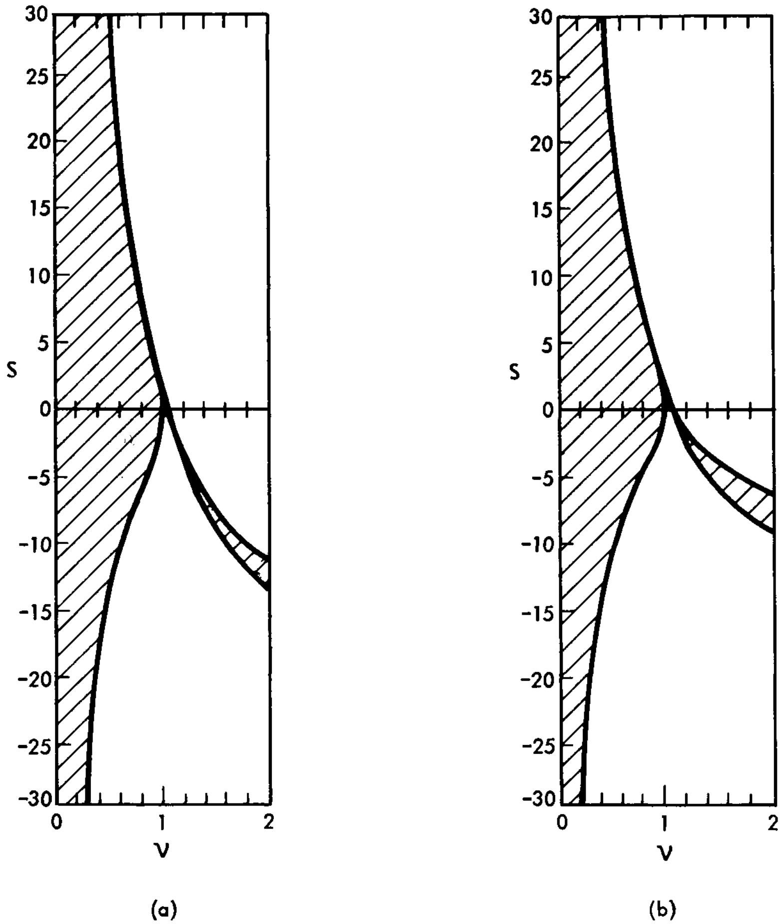

Fig. 8. Approximate attitude instability regions obtained by averaging h_i $(i = 1, 2, 3)$ over one orbit. (a) Direct orbit. (b) Retrograde orbit.

commensurate with the orbital rate. Analogously, here we say that external resonance occurs for the upper unshaded regions of Figures 8a, b whenever a pair of values of ν and s lead to two positive real solutions ω_1 and ω_2 $(\omega_2 \geqslant \omega_1)$ of Equation (74) such that

$$\omega_1 = jn/2 \quad \text{or} \quad \omega_2 = jn/2\,, \qquad (j = 1, 2, 3, \ldots) \tag{77}$$

or

$$\omega_1 + \omega_2 = jn\,, \qquad (j = 1, 2, 3, \ldots)\,, \tag{78}$$

where n, the 'mean motion' of the satellite, is given by

$$n \triangleq 2\pi/\tau^*\,. \tag{79}$$

The conditions given by Equations (77) and (78) are respectively known as 'single resonance' and 'combination resonance' (Markeev, 1967b) and correspond to two of

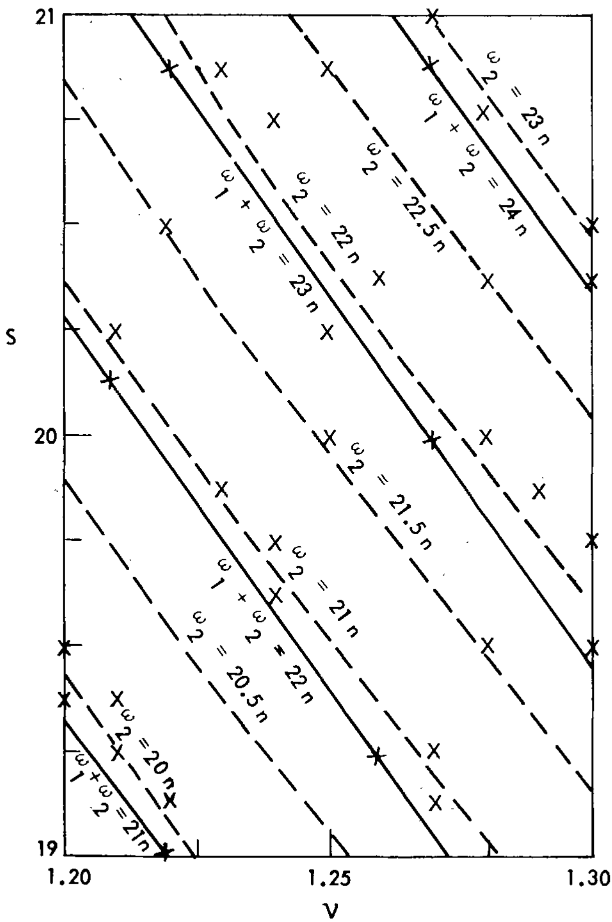

Fig. 9. Resonance lines obtained by averaging, superimposed on attitude instability chart of Figure 4.

the simplest resonance conditions of the more general form $n_1\omega_1 + n_2\omega_2 = jn$ where n_1, n_2, j are integers. Figure 9 shows approximate resonance lines superimposed on the instability chart given in Figure 4 for the direct orbit. Both types of resonances are seen to occur and, more importantly, certain of the resonance lines lie quite close to the unstable points plotted in Figures 5a–c. The specific figures and their corresponding resonance bands are

Figure 5a: $\omega_2 = 21.5n$,

Figure 5b: $\omega_2 = 22n$, $\omega_1 + \omega_2 = 23n$,

Figure 5c: $\omega_2 = 20n$, $\omega_1 + \omega_2 = 21n$.

These results suggest that a more detailed study of the relationship between orbital–attitude resonances and unstable attitude motions would be fruitful. As a first step, a Fourier analysis could be performed for the functions h_i, $(i = 1, 2, 3)$, given by

Equations (52), (53), and (54). Because of the symmetrical nature of the periodic orbits under consideration, this would yield truncated expansions of the form

$$h_i = \tilde{h}_i + \sum_{k=1}^{m} A_{ik} \cos kn\tau , \qquad (i = 1, 3) , \tag{80}$$

$$h_2 = \sum_{k=1}^{m} A_{2k} \sin kn\tau , \tag{81}$$

defined in the interval $-\tau^*/2 \leqslant \tau \leqslant \tau^*/2$. Substituting Equations (80), (81) into Equations (64), (65) would then lead to a wide variety of resonance conditions similar to those given by Equations (77), (78). Since one would expect higher frequencies to be attenuated in the functions h_1, h_2, h_3, the absolute values of the coefficients A_{ik} ($i = 1, 2, 3$; $k = 1, \ldots, m$) should become successively smaller as k becomes larger. Consequently, the effects of orbital–attitude resonances should diminish markedly with increasing k (Hitzl, 1970). However, such a detailed study of special resonances is outside the scope of the present paper.

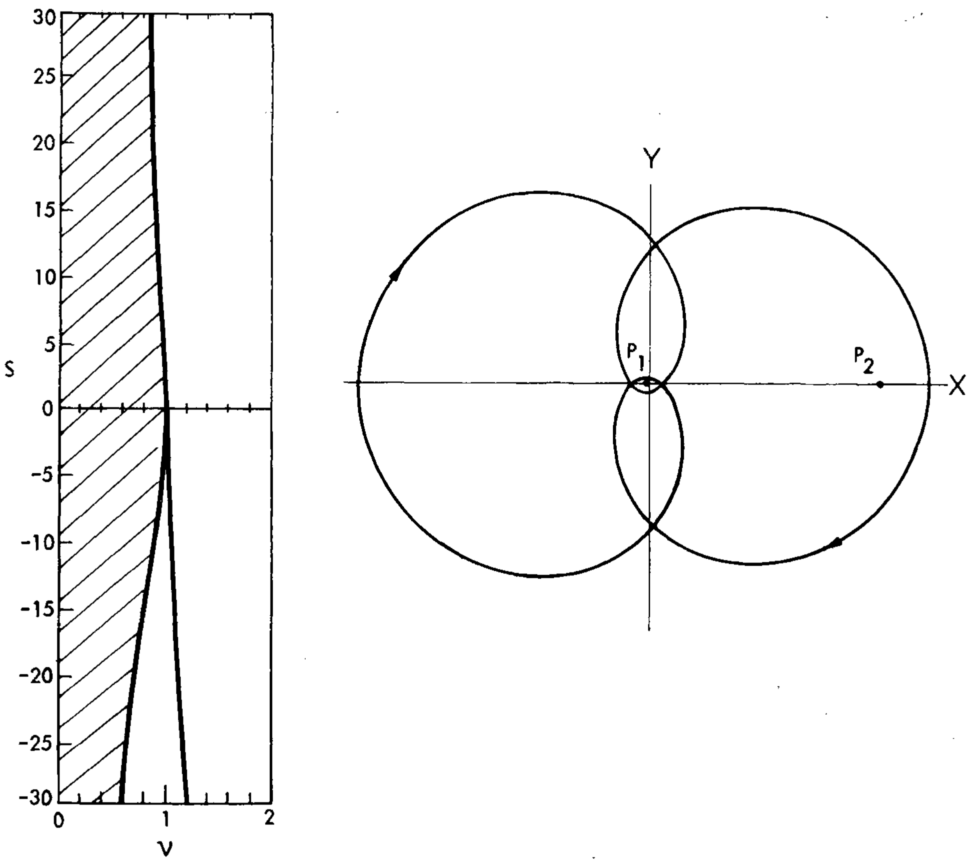

Fig. 10. Approximate attitude instability regions for a second retrograde orbit of family C_{12}.

Having seen that useful information can indeed be gleaned from this approximate analysis, we produced instability charts for several other stable periodic orbits for the Earth–Moon system ($\mu = \mu^*$) belonging to the families C_{ij} ($i = 1, 2$; $j = 2, 4, 5$) (see Hitzl and Hénon, 1977).

Results are presented in Figure 10 for one of these – a second retrograde orbit of family C_{12}. The corresponding initial conditions are

$$\bar{x}(0) = 1.2155\,,$$

$$\bar{y}(0) = \bar{x}'(0) = 0.0\,,$$

$$\bar{y}'(0) = -1.460\,949\,160\,477\,6558\,,$$

while the nondimensional period τ^* is $\tau^* = 6.292\,841\,056\,728\,9988$ and $\tilde{h}_1 = 59.935\,36$, $\tilde{h}_3 = 59.729\,34$. This orbit is of practical interest since there is an extended range of initial positions near $\bar{x}(0) = 1.2155$ yielding periodic orbits that are stable for small perturbations in the orbit plane (Hitzl, 1977). Moreover, the orbital motion is only 'slightly unstable' in the direction normal to the plane. Consequently, this orbit is a potential candidate for future space missions where relatively close passages by both the Earth and Moon are desired. Comparing Figure 10 with Figure 8, however, we find in the former a larger region of *attitude* instability due to the close passages by the Earth.

For future reference, the Jacobi constant C, and the in-plane and out-of-plane stability indices, k and k_v,† are given in Table I for the direct orbit and two retrograde orbits discussed in this paper.

TABLE I

Orbital data

	Direct orbit	First retrograde orbit	Second retrograde orbit
C	2.669 522 102 533	−0.488 771 845 180	1.059 149 117 831
k	0.778 247	−0.354 715	0.763 224
k_v	4.056 609	21.026 708	1.020 489

References

Auelman, R. R.: 1963, *AIAA J.* **1**, 1445.

Breakwell, J. V. and Pringle, R., Jr.: 1965, *Proceedings of the International Astronautical Congress*, Athens, Greece, pp. 305–325.

Debra, D. B. and Delp, R. H.: 1961, *J. Astron. Sci.* **8**, 14.

Hitzl, D. L.: 1970, 'Gravity-Gradient Attitude Perturbations of Symmetric and Tri-Axial Satellites Near Resonance', Doctoral Dissertation, Department of Aeronautics and Astronautics, Stanford University.

Hitzl, D. L.: 1972, *Celest. Mech.* **5**, 433.

† The in-plane or out-of-plane orbital motion of the satellite's mass center is unstable whenever $|k| > 1$ or $|k_v| > 1$, respectively.

Hitzl, D. L.: 1977, 'Critical Second Species Periodic Orbits in the Restricted Problem for $\mu > 0$', presented at 1977 AAS/AIAA Astrodynamics Conference, Jackson Lake Lodge, Wyoming, September 7–9; *Celest. Mech.*, under revision.

Hitzl, D. L. and Hénon, M.: 1977, *Celest. Mech.* **15**, 421.

Kane, T. R.: 1965, *AIAA J.* **3**, 726.

Kane, T. R.: 1972, *Dynamics*, Second Edition, Stanford University.

Kane, T. R. and Barba, P. M.: 1966, *J. Appl. Mech.* **33**, 402.

Kane, T. R. and Likins, P. W.: 1971, 'Kinematics of Rigid Bodies in Spaceflight', Technical Report No. 204, Department of Applied Mechanics, Stanford University.

Kane, T. R. and Likins, P. W.: 1975, 'Gravitational Forces and Moments on Spacecraft', NASA CR-2618.

Kane, T. R. and Marsh, E. L.: 1971, *Celest. Mech.* **4**, 78.

Kane, T. R. and Shippy, D. J.: 1963, *J. Astron. Sci.* **10**, 114.

Kane, T. R., Marsh, E. L., and Wilson, W. G.: 1962, *J. Astron. Sci.* **9**, 108.

Likins, P. W.: 1965, *J. Astron. Sci.* **12**, 18.

Markeev, A. P.: 1965, *Cosmic Res.* **3**, 544.

Markeev, A. P.: 1967a, *Cosmic Res.* **5**, 318.

Markeev, A. P.: 1967b, *Cosmic Res.* **5**, 457.

Pringle, R. Jr.: 1964, *AIAA J.* **2**, 908.

Szebehely, V.: 1967, *Theory of Orbits*, Academic Press, New York.

Thomson, W. T.: 1962, *J. Astron. Sci.* **9**, 31.

Wallace, F. B., Jr. and Meirovitch, L.: 1967, *AIAA J.* **5**, 1642.